

RSC Advances



This is an *Accepted Manuscript*, which has been through the Royal Society of Chemistry peer review process and has been accepted for publication.

Accepted Manuscripts are published online shortly after acceptance, before technical editing, formatting and proof reading. Using this free service, authors can make their results available to the community, in citable form, before we publish the edited article. This *Accepted Manuscript* will be replaced by the edited, formatted and paginated article as soon as this is available.

You can find more information about *Accepted Manuscripts* in the [Information for Authors](#).

Please note that technical editing may introduce minor changes to the text and/or graphics, which may alter content. The journal's standard [Terms & Conditions](#) and the [Ethical guidelines](#) still apply. In no event shall the Royal Society of Chemistry be held responsible for any errors or omissions in this *Accepted Manuscript* or any consequences arising from the use of any information it contains.

ARTICLE

Magnetic Nanoparticles Supported Oxime Palladacycle as a Highly Efficient and Separable Catalyst for Room Temperature Suzuki–Miyaura Coupling Reaction in Aqueous Media

Cite this: DOI: 10.1039/x0xx00000x

Received 00th January 2012,

Accepted 00th January 2012

DOI: 10.1039/x0xx00000x

www.rsc.org/

Mohammad Gholinejad,^{*a} Mehran Razeghi,^a and Carmen Najera^b

A novel magnetic nanoparticle-supported oxime palladacycle catalyst was successfully prepared and characterized. The magnetically recoverable catalyst was evaluated in room temperature Suzuki–Miyaura cross-coupling reaction of aryl iodides and bromides in aqueous media. The catalyst was shown to be highly active under phosphine-free and low Pd loading (0.3 mol%) conditions. The catalyst could be easily separated from the reaction mixture using an external magnet and reused for six consecutive runs without a significant loss of activity.

Introduction

Palladium catalyzed cross-coupling reactions are very important and potent strategies for the formation of carbon-carbon bonds.¹ Particularly, Suzuki–Miyaura reaction, which is the cross coupling reaction between aryl, vinyl, or alkyl halides or pseudo-halides and organoboron reagents is one of the well-known studied and advanced palladium catalyzed reactions for the formation of different types of compounds, specially biphenyls.²

Since the palladium is an expensive noble metal and also there is a possibility of contamination of the products with palladium which has high toxicity level, in the recent years, significant progress in heterogenization of palladium catalysts have been achieved. Even with substantial progress in this area, separating of the catalyst from the reaction medium by conventional methods such as filtration or centrifugation is not an easy task.³ One way to solve this problem, is using magnetic nanoparticles (MNPs) with large ratio of surface area to volume, superparamagnetic behavior and low toxicity as a support for stabilization of metal catalysts.⁴ Along this line, in recent years, extensive attention has been paid to use of magnetic nanoparticles as a promising support for stabilization of palladium catalysts and their application in different carbon-carbon bond forming reactions.⁵

Among the different types of palladium catalysts, oxime-based palladacycles are one of the most promising, efficient and easily prepared catalysts for carbon-carbon bond forming

reactions as source of Pd clusters⁶ or NPs.⁷ Though, the efficiency of oxime palladacycles, these catalysts suffers from problems associate to the homogenous catalysts. In recent years, few attempts have been made to solve the problem by immobilization of oxime palladacycles on different supports.⁸ Polystyrene,⁹ [poly(ethyleneglycol) dimethacrylate],¹⁰ and other resins,^{10,11} silica,¹² and periodic mesoporous organosilica (PMO),¹³ phosphonium tagged,¹⁴ and self-supported oxime palladacycles¹⁵ are different strategies which have been used for heterogenization of oxime palladacycles. However to the best of our knowledge, there are no reports dealing with immobilization of oxime palladacycles on magnetic nanoparticles.

Recently, we have reported application of magnetite nanoparticles as an efficient catalyst for Sonogashira–Hagihara reaction under heterogeneous and ligand-free conditions in ethylene glycol.¹⁶

Herein, for the first time, we report the use of magnetic nanoparticles as a catalyst support for immobilization of oxime palladacycles and its application in room temperature Suzuki–Miyaura cross-coupling reaction in aqueous media.

Results and discussion

Magnetic Fe₃O₄ nanoparticles were prepared without using any capping agent or surfactant *via* conventional co-precipitation of FeCl₂ and FeCl₃ according to the reported methods.^{16–17} TEM

image of prepared Fe_3O_4 nanoparticles showed the formation of mono-dispersed and uniform Fe_3O_4 nanoparticles in average size of 10-15 nm (Figure 1).

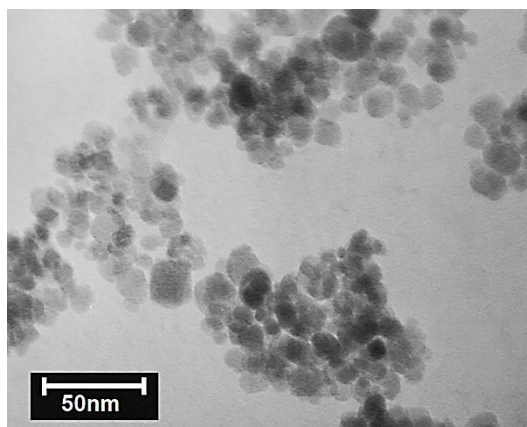
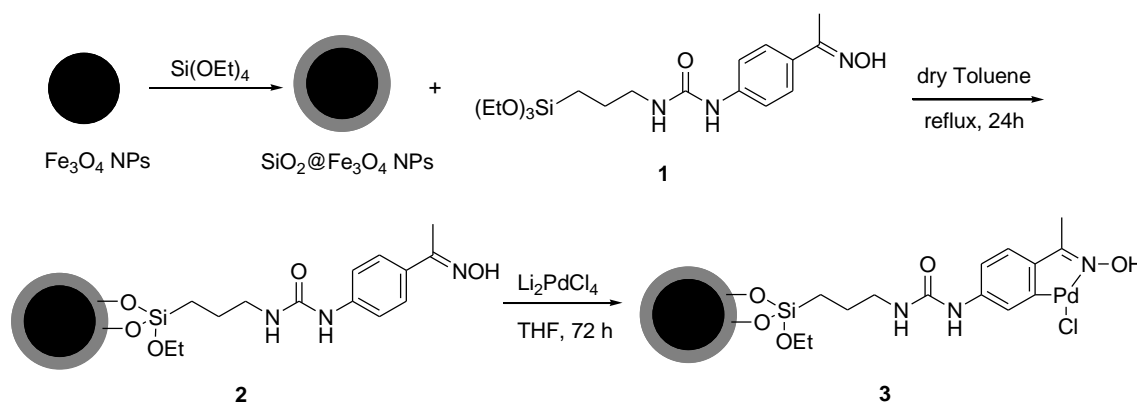


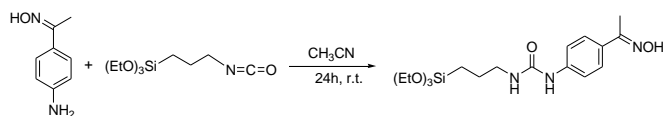
Fig. 1 TEM image of prepared Fe_3O_4 nanoparticles

The obtained Fe_3O_4 nanoparticles were coated with a thin layer of silica using a sol-gel process to give core/shell Fe_3O_4 nanoparticles ($\text{SiO}_2@ \text{Fe}_3\text{O}_4$ NPs). The obtained silica-coated Fe_3O_4 nanoparticles were characterized using FT-IR analysis which showed the Si-O-Fe bond in 1097 cm^{-1} (Figure 1, supporting information). The oxime can be easily anchored onto the surface of the $\text{SiO}_2@ \text{Fe}_3\text{O}_4$ by using synthesized 1-(4-(1-(hydroxyimino)ethyl)phenyl)-3-(3-(triethoxysilyl)propyl)urea (**1**) obtained from reaction of 1-(4-aminophenyl)ethanone oxime and triethoxy(3-isocyanatopropyl) silane (Scheme 1)



Scheme 1 Synthesis of oxime supported $\text{SiO}_2@ \text{Fe}_3\text{O}_4$ NPs **3**.

Formation of oxime **1** was confirmed using ^1H NMR from the reaction mixture of 1-(4-aminophenyl)ethanone oxime and triethoxy (3-isocyanatopropyl) silane (Scheme 2). ^1H NMR showed complete reaction of 1-(4-aminophenyl)ethanone oxime and formation of 1-(4-(1-(hydroxyimino)ethyl)phenyl)-3-(3-(triethoxysilyl)propyl)urea which was approved by downfield shift of protons of oxime product compared to starting oxime (Figure 2, supporting information).



Scheme 2 Synthesis of 1-(4-(1-(hydroxyimino)ethyl)phenyl)-3-(3-(triethoxysilyl)propyl)urea **1**.

Loading of oxime on $\text{SiO}_2@ \text{Fe}_3\text{O}_4$ was determined using elemental analysis, which showed 0.41 mmol oxime per gram Fe_3O_4 NPs. In addition TG analysis of supported oxime **2** confirmed the presence of organic group with 0.38 mmol g^{-1} (Figure 2). The final oxime palladacycle catalyst **3** was

obtained simply by dissolving Li_2PdCl_4 in MeOH and treating it with the oxime-functionalized $\text{SiO}_2@ \text{Fe}_3\text{O}_4$, with a loading of 0.32 mmol g^{-1} determined by ICP analysis. FT-IR analysis of catalyst showed presence of (C=O) bond of catalyst as well as (Fe-O-Si) bonds shift at 1634 and 1090 cm^{-1} respectively (Figure 3, supporting information). Also, the presence of palladium in the structure of catalyst was confirmed by energy-dispersive X-ray spectroscopy (EDX) (Figure 3) obtained from SEM analysis (Figure 4) of catalyst **3**. It is worth mentioning that SEM image confirm uniform and regular morphology of the catalyst structure.

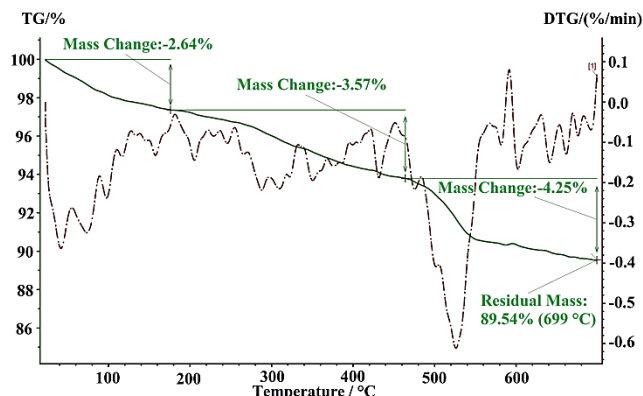


Fig. 2 Thermogravimetric diagram of the the catalyst.

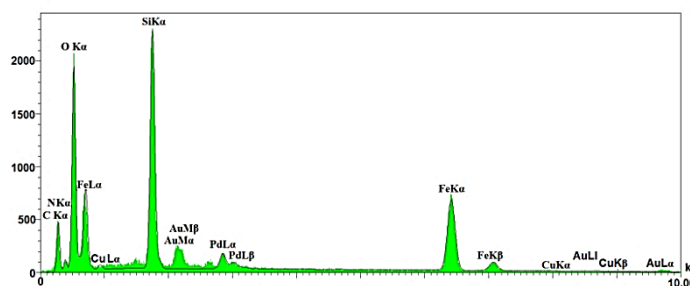


Fig. 3 EDX spectrum of the catalyst

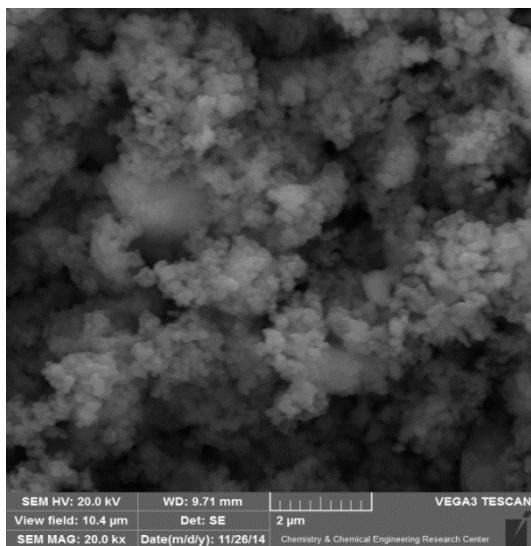


Fig. 4 SEM image of the catalyst

The superparamagnetic performance of the catalyst was confirmed using magnetization curves of Fe_3O_4 NPs, $\text{SiO}_2@ \text{Fe}_3\text{O}_4$ NPs, and final oxime palladacycle supported catalyst at room temperature (Figure 5). Zero coercivity and remanence on the magnetization loop was observed in all three samples without presence of hysteresis loop. These results indicated the superparamagnetic property and the ability of the material to be separated from the reaction mixture by an external magnet (Figure 5). In addition, the decrease in the magnetization value of the $\text{SiO}_2@ \text{Fe}_3\text{O}_4$ (35 emu g^{-1}) in comparison with Fe_3O_4 NPs (60 emu g^{-1}) confirms that the silica

coating and formation of core/shell nanoparticles. Furthermore, a decreases in the magnetization value of the final catalyst **3**, confirm immobilization of oxime palladacycle on core/shell $\text{SiO}_2@ \text{Fe}_3\text{O}_4$ NPs.

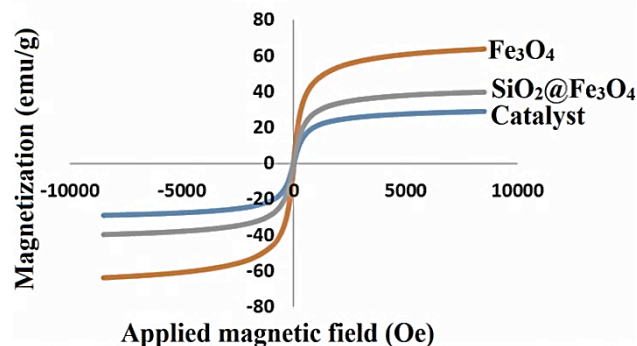


Fig. 5 Magnetization curves Fe_3O_4 NPs, $\text{SiO}_2@ \text{Fe}_3\text{O}_4$ and catalyst

The nitrogen adsorption–desorption isotherms for $\text{SiO}_2@ \text{Fe}_3\text{O}_4$, supported oxime **2** and catalyst **3** are shown in Figure 6 and the physical parameters measured with N_2 sorption are summarized in Table 1.

The results indicated that all samples possesses type-IV isotherms with H3 hysteresis loop. The BET surface area and pore volume decreased in $\text{SiO}_2@ \text{Fe}_3\text{O}_4$ compared with oxime **2** which may be attributed to the possibility that the pores of SiO_2 were partially covered by the grafting oxime **1** (Table 1). Also, the results indicated that surface area and pore volume increased after introducing of palladium particles. This may be related to complex formation of oxime palladacycle which caused increasing in surface area and porous property of the catalyst. Despite the low surface area of the catalyst, high catalytic activity of catalyst (**3**) is may related to distribution of the nanoparticles on the surface.

Moreover, pore size distributions calculated from the adsorption branch using BJH method displayed uniform which centered on around 6 nm (Table 1).

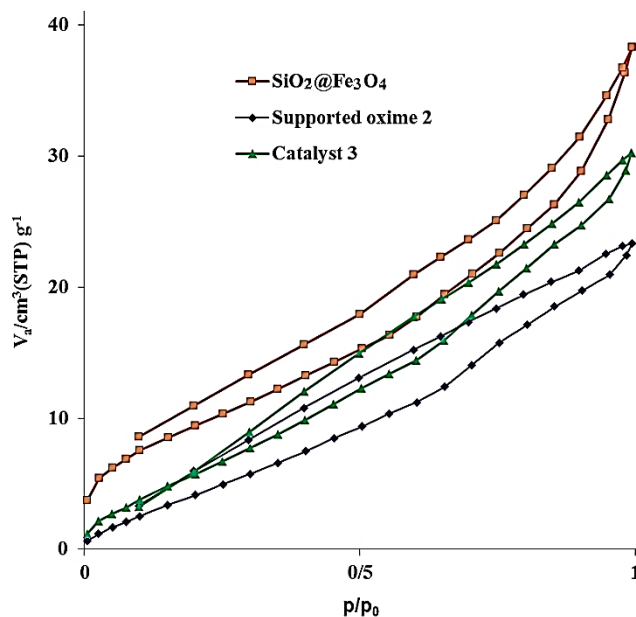


Fig. 6 N₂ adsorption/desorption isotherms of SiO₂@Fe₃O₄, supported oxime palladacycle **2** and catalyst **3**

Table 1. The BET surface area, BJH pore volume and pore size for SiO₂@Fe₃O₄, supported oxime palladacycle **2** and catalyst **3**

Sample	S _{BET} ^a (m ² g ⁻¹)	V _t ^b (cm ³ g ⁻¹)	D _{BJH} ^c (nm)
SiO ₂ @Fe ₃ O ₄	36	8.2	6.4
Supported oxime 2	23	5.4	6.02
Catalyst 3	28	6.6	6.4

It is worth mentioning that we have prepared catalyst **3** using different ratio of Si/Pd and used them in the reaction of 4-bromoanisole and phenylboronic acid. However, results indicated no appreciate difference in catalytic activity of catalysts (Table 1, supporting information).

In order to find information about state of palladium in the catalyst **3**, we studied solid UV spectrum of catalyst and Li₂PdCl₄ as a source of Pd(II) species (Figure 4, supporting information). Results showed a peak at 324 nm for catalyst **3** which is very similar to Pd(II) peak in Li₂PdClO₄. This observation confirmed formation of Pd(II) oxime palladacycle complex in the catalyst.

The catalytic activity of prepared catalyst **3** was assessed in Suzuki-Miyaura coupling reaction. In order to find optimal reaction conditions, a less reactive 4-bromoanisole and phenylboronic acid were selected as substrates for a model reaction (Table 2). Initially, the reaction was studied under different solvents using K₂CO₃ as base at 25-60 °C (Table 2, entries 1-9). Using aqueous ethanol (1:1) the reaction took place quantitatively in only 1 h (Table 2, entry 6). However, working at 25 °C the reaction needed 1 d to give 4-methoxybiphenyl in 84% yield (Table 2, entry 9). When the reaction was performed in aqueous ethanol with different organic and inorganic bases (Table 2, entries 10-16), *t*-BuOK gave the highest 97% GC yield (Table 2, entry 14).

Table 2 Screening of different reaction conditions for the reaction of 4-bromoanisole with phenylboronic acid in the presence of catalyst.^a

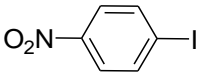
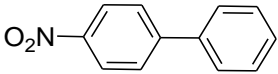
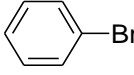
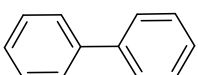
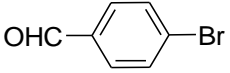
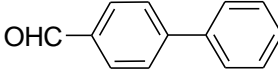
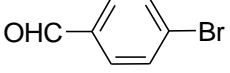
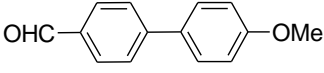
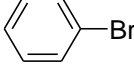
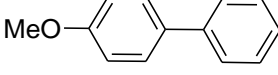
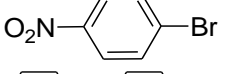
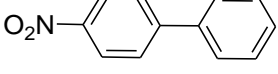
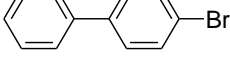
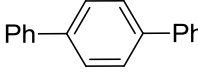
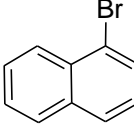
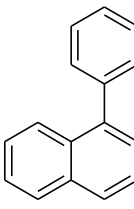
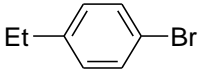
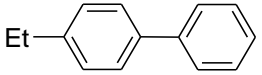
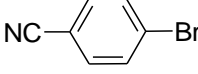
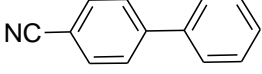
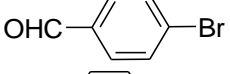
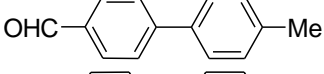
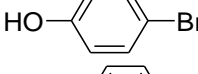
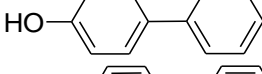
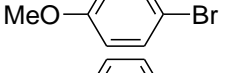
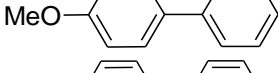
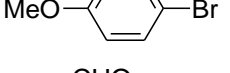
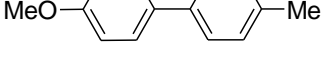
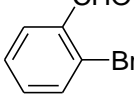
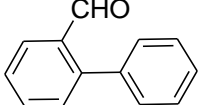
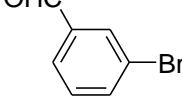
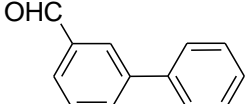
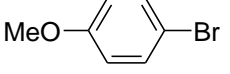
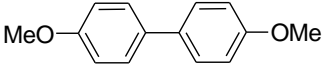
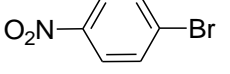
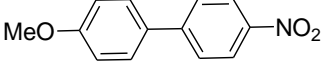
Entry	Base	Solvent	Temp. (°C)	Time (h)	Yield(%) ^b
1	K ₂ CO ₃	H ₂ O	60	15	91
2	K ₂ CO ₃	Toluene	60	15	7
3	K ₂ CO ₃	DMF	60	15	2
4	K ₂ CO ₃	CH ₃ CN	60	15	7
5	K ₂ CO ₃	THF	60	15	1
6	K ₂ CO ₃	H ₂ O/EtOH	60	1	100
7	K ₂ CO ₃	EtOH	60	5	90
8	K ₂ CO ₃	H ₂ O/EtOH	50	2	78 ^c
9	K ₂ CO ₃	H ₂ O/EtOH	25	24	84
10	Et ₃ N	H ₂ O/EtOH	25	24	5
11	DABCO	H ₂ O/EtOH	25	24	49
12	NaOAc	H ₂ O/EtOH	25	24	12
13	K ₃ PO ₄	H ₂ O/EtOH	25	24	86
14	<i>t</i> -ButOK	H ₂ O/EtOH	25	24	97
15	<i>t</i> -ButOK	H ₂ O	25	24	70
16	<i>t</i> -ButOK	EtOH	25	24	88

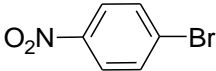
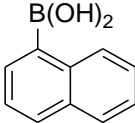
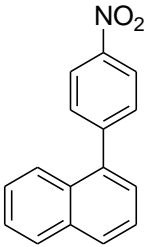
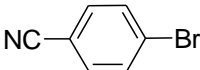
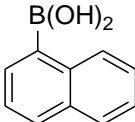
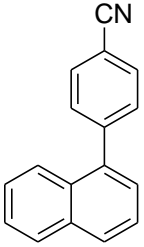
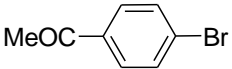
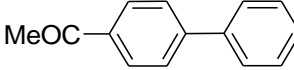
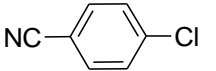
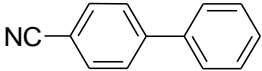
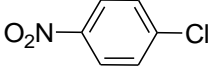
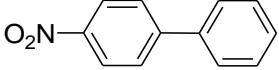
^a Reaction conditions: 4-bromoanisole (1 mmol), phenylboronic acid (1.5 mmol), base (1.5 mmol), solvent (2 mL), catalyst (0.3 mol% Pd). ^b GC yields. ^c 0.1 mol% Pd

With the optimized reaction conditions in hand, *t*-BuOK as base, EtOH:H₂O (1:1) as solvent and 0.3 mol% catalyst, the substrate scope of the Suzuki-Miyaura reaction was investigated for the reaction of structurally different aryl halides with arylboronic acids (Table 3).

Table 3 Suzuki cross-coupling of structurally different aryl halides and arylboronic acids.^a

Entry	Ar ¹	Ar ²	Time (h)	Product	Yield (%) ^b
1		Ph	0.3 (1)		95(100)
2		Ph	0.7		99
3		Ph	0.7		92
4		Ph	1		92
5		Ph	0.3(1)		92(98)

6		Ph	1		96
7		Ph	18		85
8		Ph	1		100
9		4-MeOC ₆ H ₄	2		100
10		4-MeOC ₆ H ₄	12 (24)		90 (98)
11		Ph	10		93
12		Ph	24		95
13		Ph	17		98
14		Ph	17		98
15		Ph	1		99
16		4-MeC ₆ H ₄	1		99
17		Ph	24		97
18		Ph	24		95
19		4-MeC ₆ H ₄	24		83
20		Ph	24		70
21		Ph	24		98
22		4-MeOC ₆ H ₄	24		91
23		4-MeOC ₆ H ₄	3		98

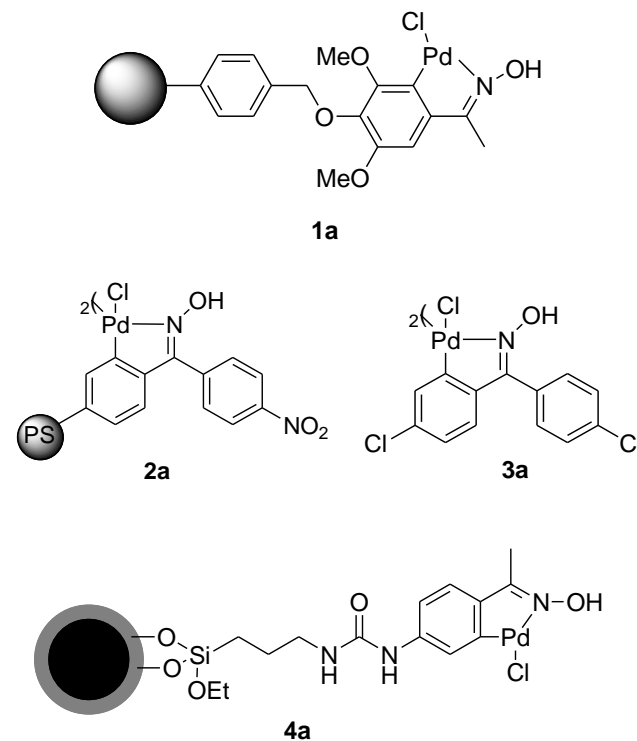
24			5		96
25			1		95
26		Ph	2		97
27		Ph	24		67 ^c
28		Ph	24		48 ^c

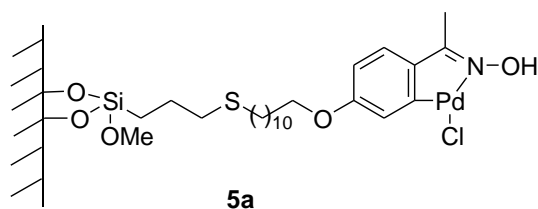
^aReaction conditions: 4-bromoanisole (1 mmol), phenylboronic acid (1.5 mmol), base (1.5 mmol), solvent (2 mL), catalyst (0.3 mol%). ^bYields are isolated. ^cReactions were performed at 60 °C.

As shown in Table 3, the coupling reaction between aryl iodides and phenylboronic containing electron-donating groups (Table 2, entries 3-5) as well as nitro group (Table 3, entry 6) and thienyl iodide (Table 3, entry 2), proceeded effectively to afford the corresponding products in excellent yields. Also, reactions of wide range of aryl bromides containing both electron-donating and electron-withdrawing groups with different arylboronic acids proceeded well and desired coupling products were obtained in high to excellent isolated yields. It is worth mentioning that reaction of a less reactive 4-bromophenol at room temperature afforded 4-hydroxybiphenyl in 97% yield (Table 3, entry 17). Different substituted arylboronic acids like 4-methoxyphenyl, 4-tolyl and 1-naphthylboronic acids gave good yields (Table 3, entries 9, 10, 16, 19, and 22-25). All attempts to carry out the reaction of aryl chlorides under optimized reaction conditions were unsuccessful. However, increasing the reaction temperature to 60 °C, 4-chloro-benzonitrile and nitrobenzene reacted with phenylboronic acid to give the corresponding 4-ciano and 4-nitrobiphenyl in 67 and 48% yield, respectively (Table 3, entries 27 and 28).

Comparison catalytic activity of presented catalyst with other supported oxime palladacycles such as polymer supported oxime palladacycles 1a¹¹ and 2a^{10a} and also unsupported oxime palladacycle 3a^{7b} (scheme 3) in Suzuki coupling reaction of 4-bromoanisole with phenylboronic acid as a common substrate, showed noticeably efficiency of presented magnetic supported oxime palladacycle (Table 4, entries 1-7). We have also compared catalytic activity of magnetic supported oxime palladacycle with silica supported oxime palladacycle 5a¹² reported by Corma and coworkers in the reaction of 4-bromoacetophenone with phenylboronic acid as a common

substrate. The result indicated that using 4a reaction proceeded under lower Pd loading and temperature with almost similar yields (Table 4, entries 8-10).





Scheme 3 Different oxime palladacycles reported in Suzuki coupling reaction.

Table 4 Comparison catalytic activity of magnetic supported oxime palladacycle with other reported oxime palladacycles.

Entry	Catalyst	Temp. (°C)	Time (h)	Pd (mol%)	Yield%
1	1a	50	2	1	96
2	1a	50	2	0.1	62
3	2a	100	24	0.1	89
4	3a	110	2	0.01	94
5	4a	60	1	0.3	100
6	4a	25	24	0.3	95
7	4a	50	2	0.1	78
8	4a	25	2	0.3	97
9	4a	60	0.1	0.3	95
10	5a	100	0.1	0.65	99

The recovery and reuse of catalyst becomes a main factor from the point of view of economic and environmental sustainability. Along this line, we have studied recyclability of magnetic nanoparticles supported oxime palladacycle catalyst for the reaction of less reactive 4-bromoanisole with phenylboronic acid under the optimized reaction conditions. After the completion of the reaction, the magnetic catalyst could be simply recovered from the reaction mixture using an external magnet, washed with water and diethyl ether, dried under vacuum and reused in another batch. Recycling experiments indicated that the catalyst **3** can be successfully used during six consecutive runs without a significant loss of activity (Figure 7).

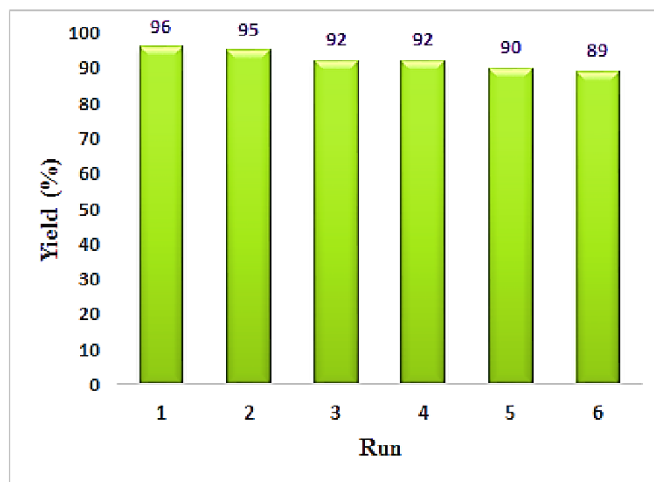
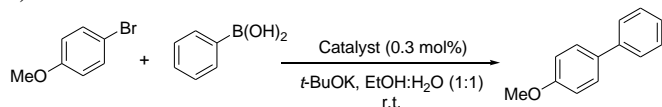


Fig. 7 Recycling of catalyst **3** for the reaction of 4-bromoanisole with phenylboronic acid.

Atomic absorption spectroscopy (AAS) of the solution obtained after isolation of catalyst in the first run showed the amount of leaching of Pd was 1.6%. Also, amount of palladium in the recycled catalyst after 3rd run determined by ICP analysis to be 0.29 mmol g⁻¹. In order to get information about stability of the catalyst, TGA analysis of recycled catalyst after 3rd run was studied. The results showed that the catalyst is thermally stable up to 200 °C and organic functional group containing oxime palladacycle was presented in the structure of the catalyst (Figure 5, supporting information).

Furthermore, electron dispersive X-ray (EDX) of the recycled catalyst after a 3rd run confirmed the presence of Fe and Pd species in the structure of the recovered catalyst (Figure 8).

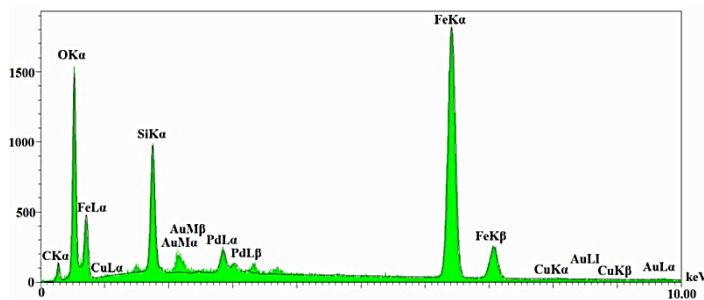


Fig. 8 EDX spectrum of the catalyst **3** after the 3rd run.

Conclusions

In conclusion, new magnetic nanoparticle-supported oxime palladacycle catalyst was successfully prepared and characterized. Using this catalyst, structurally different aryl iodides and bromides were reacted effectively with arylboronic acids in aqueous media at room temperature. The magnetically separable and phosphine free catalyst was successfully recycled and used in six consecutive runs with similar catalytic activity.

Experimental Section

General

All chemicals were purchased from Sigma-Aldrich, Acros and Merck and were used without further purification. Thin layer chromatography was carried out on silica gel 254 analytical

sheets obtained from Fluka. ^1H NMR spectra were recorded at 400 MHz and ^{13}C NMR spectra were recorded at 100 MHz in CDCl_3 using TMS as internal standard. Thermogravimetric analysis (TGA) was conducted from room temperature to 700 °C in an oxygen flow using a NETZSCH STA 409 PC/PG instrument. FT-IR spectra were recorded on a Bruker Vector 22. Energy dispersive X-ray analysis (EDX) was obtained using Carl Zeiss SiGMA instrument. The structures of the prepared materials were observed by transmission electron microscopy (Philips CM-120). Adsorption-desorption analyses were recorded using (BELSORP-max (Japan)).

Synthesis of Fe_3O_4 nanoparticles:

Magnetite (Fe_3O_4) nanoparticles were prepared following a similar procedure reported in the literature,¹⁷ which will briefly be explained in the following. $\text{FeCl}_3 \cdot 6(\text{H}_2\text{O})$ (11.0 g) and $\text{FeCl}_2 \cdot 4(\text{H}_2\text{O})$ (4.0 g) were dissolved in 250 mL deionized water under argon with vigorous stirring using mechanical stirrer. To the mixture aqueous ammonia (25%, 40 mL) was added slowly over 20 min under argon atmosphere and mixture was stirred at 80 °C for 4 h. A black precipitate (Fe_3O_4) were collected by external magnet and washed three times with deionized water and ethanol and dried under vacuum.

Synthesis of silica-coated Fe_3O_4 nanoparticles

1.0 g of synthesized Fe_3O_4 nanoparticles was sonicated in ethanol (200 mL) for 30 min at room temperature. Then, to the resulting suspension were added 2 mL of tetraethyl orthosilicate (TEOS) and 6 mL aqueous ammonia and mixture was stirred for 24 h at room temperature. Obtained silica-coated Fe_3O_4 nanoparticles were separated by an external magnet and washed with H_2O (3×10 mL) and EtOH (3×10 mL) and dried under vacuum.

Synthesis of 1-(4-aminophenyl)ethanone oxime

4-aminoacetophenone (1 mmol, 0.135 g) was dissolved in mixture of 2 mL H_2O and 0.5 mL EtOH at 70 °C. Then, NaOAc (3 mmol, 0.246 g) and hydroxylamine hydrochloride (2 mmol, 0.140 g) were added and mixture was stirred for 1 h at 70 °C. Then, reaction mixture was cooled to 0 °C in an ice bath to precipitate the desired oxime product. The mixture was filtered and obtained oxime was dried under a vacuum.

Synthesis of 1-(4-(1-(hydroxyimino)ethyl)phenyl)-3-(3-(triethoxysilyl)propyl)urea (1)

To 10 mL flask containing 1-(4-aminophenyl)ethanone oxime (1 mmol) was added 5 mL dry acetonitrile and mixture was stirred at room temperature. Then triethoxy(3-isocyanatopropyl)silane (1.5 mmol) was added under argon protection and solution was stirred under argon atmosphere for 48 h at room temperature. Evaporation of solvent provided the crude 1-(4-(1-(hydroxyimino)ethyl)phenyl)-3-(3-(triethoxysilyl)propyl)urea (1).

Synthesis of oxime-functionalized MNP (2)

Silica-coated Fe_3O_4 nanoparticles (500 mg) were sonicated in 20 mL dry toluene and above obtained crude oxime product (1) was added and mixture was refluxed for 24 h under argon atmosphere. Then, the reaction mixture was subjected to magnetic separation, and obtained product (2) was washed sequentially with H_2O (3×10 mL) and CH_3CN (3×10 mL) and finally dried under vacuum.

Synthesis of MNP supported oxime palladacycle (3)

400 mg of compound 2 was sonicated at 5 mL MeOH for 30 min at room temperature. Then, Li_2PdCl_4 (0.075 mmol, 0.02 g) and NaOAc (0.5 mmol, 0.041 g) were added. The mixture was stirred under argon atmosphere for 72 h at room temperature.

Then, reaction mixture was subjected to magnetic separation, and isolated material was washed sequentially with H_2O (3×10 mL) and EtOH (3×10 mL) and dried under vacuum for 24 h.

General procedure for Suzuki-Miyaura reaction:

In a 10 mL flask, aryl halide (1 mmol), arylboronic acid (1.5 mmol), *t*-ButOK (1.5 mmol), catalyst (0.3 mol%) and 2 mL water/ethanol (1:1) were added and stirred using mechanical stirrer at r.t. to 60 °C (with respect to aryl halide). The progress of the reactions were monitored by GC. After completion of the reaction, the crude product was extracted using ethyl acetate. The further purification was achieved by column chromatography on silica using the hexane and ethyl acetate as eluent.

Acknowledgements

The authors are grateful to Institute for Advanced Studies in Basic Sciences (IASBS) Research Council and Iran National Science Foundation (INSF-Grant number of 93020713) for support of this work.

Notes and references

^aDepartment of Chemistry, Institute for Advanced Studies in Basic Sciences (IASBS), P. O. Box 45195-1159, Gavazang, Zanjan 45137-6731, Iran.

^bDepartamento de Química Orgánica and Centro de Innovación en Química Avanzada (ORFEO CINQA), Universidad de Alicante, Apdo. 99, E-03080 Alicante, Spain

Electronic Supplementary Information (ESI) available: [details of any supplementary information available should be included here]. See DOI: 10.1039/b000000x/

- (a) Á. Molnár, in *Palladium-Catalyzed Coupling Reactions: Practical Aspects and Future Developments*, Wiley-VCH Verlag, Weinheim, 2013; (b) Á. Molnár, *Chem. Rev.* 2011, 111, 2251; (c) R. Jana, T. P. Pathak and M. S. Sigman, *Chem. Rev.* 2011, 111, 1417; (d) M. Lamblin, L. Nassar-Hardy, J. C. Hierso, E. Fouquet and F. X. Felpin, *Adv. Synth. Catal.* 2010, 352, 33; (e) B. C. G. Söderberg, *Coord. Chem. Rev.* 2003, 241, 147.
- (a) A. Suzuki, *J. Organomet. Chem.* 1999, **576**, 147; (b) S. Kotha, K. Lahiri and D. Kashinath, *Tetrahedron* 2002, **58**, 9633; (c) J. Hassan, M. Sévignon, C. Gozzi, E. Schulz and M. Lemaire, *Chem. Rev.* 2002, **102**, 1359; (d) F. Alonso, I. P. Beletskaya and M. Yus, *Tetrahedron* 2008, **64**, 3047; (e) V. Polshettiwar, A. Decottignies, C. Len and A. Fihri, *ChemSusChem* 2010, **3**, 502; (f) D. A. Alonso and C. Najera, *Chem. Soc. Rev.* 2010, **39**, 2891; (g) R. Rossi, F. Bellina and M. Lessi, *Adv. Synth. Catal.* 2012, **354**, 1181; (h) M. Blangetti, H. Rosso, C. Prandi and A. Deagostino, P. Venturello, *Molecules* 2013, **18**, 1188.
- (a) N. T. S. Phan, M. Van Der Sluys, and C. W. Jones, *Adv. Synth. Catal.* 2006, **348**, 609; (b) L. Yin and J. Liebscher, *Chem. Rev.* 2007, **107**, 133; (c) M. Lamblin, L. Nassar-Hardy, J.-C. Hierso, E. Fouquet and F.-X. Felpin, *Adv. Synth. Catal.* 2010, **352**, 33; (d) M. Mora, C. Jiménez-Sanchidrián and J. R.

- Ruiz, *Curr. Org. Chem.* 2012, **16**, 1128; (e) L. Djakovitch and F.-X. Felpin, *ChemCatChem* 2014, **6**, 2175.
4. (a) C. W. Lim and S. Lee, *Nano Today* 2010, **5**, 412; (b) S. Shylesh, V. Schunemann and W. R. Thiel, *Angew. Chem. Int. Ed.* 2010, **49**, 3428; (c) D. Zhang, C. Zhou, Z. Sun, L.-Z. Wu, C.-H. Tunga and T. Zhang, *Nanoscale* 2012, **4**, 6244; (d) T. Zeng, W.-W. Chen, C. M. Cirtiu, A. Moores, G. Song and C.-J. Li, *Green Chem.* 2010, **12**, 570.
5. (a) J. Kim, J. E. Lee, J. Lee, Y. Jang, S.-W. Kim, K. An, J. H. Yu and T. Hyeon, *Angew. Chem. Int. Ed.* 2006, **45**, 4789; (b) Z. Yinghuai, S. C. Peng, A. Emi, S. Zhenshun, Monalisa and R. A. Kemp, *Adv. Synth. Catal.* 2007, **349**, 1917; (c) C. G. Tan and R. N. Grass, *Chem. Commun.* 2008, 4297; (d) S. Shylesh, L. Wang and W. R. Thiel, *Adv. Synth. Catal.* 2010, **352**, 425; (e) D. Yuan, Q. Zhang and J. Dou, *Catal. Commun.* 2010, **11**, 606; (f) R. Cano, D. J. Ramón and M. Yus, *Tetrahedron* 2011, **67**, 5432; (g) R. Cano, M. Yus and D. J. Ramón, *Tetrahedron* 2011, **67**, 8079; (h) P. Li, L. Wang, L. Zhang and G.-W. Wang, *Adv. Synth. Catal.* 2012, **354**, 1307; (i) L. Zhang, P. Li, H. Li and L. Wang, *Catal. Sci. Technol.* 2012, **2**, 1859; (j) M. Ma, Q. Zhang, D. Yin, J. Dou, H. Zhang and H. Xu, *Catal. Commun.* 2012, **17**, 168; (k) X. Jin, K. Zhang, J. Sun, J. Wang, Z. Dong and R. Li, *Catal. Commun.* 2012, **26**, 199; (l) D. Rosario-Amorin, M. Gaboyard, R. Clerac, L. Vellutini, S. Nlate and K. Heuze, *Chem. Eur. J.* 2012, **18**, 3305; (m) R. Cano, M. Yus and D. J. Ramón, *Tetrahedron* 2012, **68**, 1393; (n) L. M. Rossi, N. J. S. Costa, J. Limberger and A. L. Monteiro In *Nanocatalysis Synthesis and Applications*, V. Polshettiwar and T. Asefa, Eds., Wiley: Hoboken, 2013; (o) Z. Wang, Y. Yu, Y. X. Zhang, S. Z. Li, H. Qian, and Z. Y. Lin, *Green Chem.*, 2015, **17**, 413; (p) J. Yang, D. Wang, W. Liu, X. Zhang, F. Bian, and W. Yu, *Green Chem.* 2013, **15**, 3429; (q) B. R. Vaddula, A. Saha, J. Leazer and R. S. Varma, *Green Chem.* 2012, **14**, 2133; (r) H. Firouzabadi, N. Iranpoor, M. Gholinejad, S. Akbarian, N. Jeddi, *RSC Adv.* 2014, **4**, 17060.
6. A. Leyva-Pérez, J. Oliver-Meseguer, P. Rubio-Marqués and A. Corma, *Angew. Chem. Int. Ed.* 2013, **52**, 11554.
7. (a) D. A. Alonso, C. Nájera and M. C. Pacheco, *Org. Lett.* 2000, **2**, 1823; (b) D. A. Alonso, C. Nájera and M. C. Pacheco, *J. Org. Chem.* 2002, **67**, 5588; (c) L. Botella and C. Nájera, *Angew. Chem. Int. Ed.* 2002, **41**, 179; (d) L. Botella and C. Nájera, *J. Organomet. Chem.* 2002, **663**, 46; (e) S. Iyer and A. Jayanthi, *Synlett* 2003, 1125; (f) L. Botella and C. Nájera, *Tetrahedron Lett.* 2004, **45**, 1833; (g) E. Alacid and C. Nájera, *Eur. J. Org. Chem.* 2008, 3102; (h) E. Alacid and C. Nájera, *Org. Lett.* 2008, **10**, 5011; (i) D. A. Alonso, J. F. Cívicos and C. Nájera, *Synlett* 2009, 3011; (j) J. F. Cívicos, D. A. Alonso and C. Nájera, *Adv. Synth. Catal.* 2012, **354**, 2771; (k) J. F. Cívicos, M. Gholinejad, D. A. Alonso and C. Nájera, *Chem. Lett.* 2011, **40**, 907; (l) J. F. Cívicos, D. A. Alonso and C. Nájera, *Adv. Synth. Catal.* 2011, **353**, 1683; (m) G. Zhang, X. Zhao, Y. Yan and C. Ding, *Eur. J. Org. Chem.* 2012, 669.
8. R. Ratti, *Can. Chem. Trans.* 2014, **2**, 467.
9. C.-A. Lin and F.-T. Luo, *Tetrahedron Lett.* 2003, **44**, 7565.
10. (a) E. Alacid and C. Nájera, *J. Organomet. Chem.* 2009, **694**, 1658; (b) E. Alacid and C. Nájera, *ARKIVOC* 2008, **8**, 50.
11. H.-J. Cho, S. Jung, S. Kong, S.-J. Park, S.-M. Lee and Y.-S. Lee, *Adv. Synth. Catal.* 2014, **356**, 1056.
12. C. Baleizao, A. Corma, H. García and A. Leyva, *Chem. Commun.* 2003, 606.
13. A. Corma, A. D. Das, H. García and H. A. Leyva *J. Catal.* 2005, **229**, 322.
14. J. J. Tindale and P. J. Ragogna, *Can. J. Chem.* 2010, **88**, 27.
15. (a) Q.-P. Liu, Y.-C. Chen, Y. Wu, J. Zhu and J.-G. Deng, *Synlett* 2006, 1503; (b) Y.-C. Yang and P. H. Toy, *Synlett.* 2014, **25**, 1319.
16. H. Firouzabadi, N. Iranpoor, M. Gholinejad and J. Hoseini, *Adv. Synth. Catal.* 2011, **353**, 125.
17. Q. Zhang, H. Su, J. Luo, Y. Wei, *Catal. Sci. Technol.* 2013, **3**, 235.